

# Phosphatase models: Synthesis, structure and catalytic activity of zinc complexes derived from a phenolic Mannich-base ligand



Ria Sanyal<sup>a</sup>, Prateeti Chakraborty<sup>a</sup>, Ennio Zangrando<sup>b,\*</sup>, Debasis Das<sup>a,\*</sup>

<sup>a</sup> Department of Chemistry, University of Calcutta, 92, A. P. C. Road, Kolkata 700009, India

<sup>b</sup> Department of Chemical and Pharmaceutical Sciences, University of Trieste, Via L. Giorgieri 1, 34127 Trieste, Italy

## ARTICLE INFO

### Article history:

Received 20 December 2014

Accepted 10 May 2015

Available online 19 May 2015

### Keywords:

Mannich-base

Zinc(II)

Phosphatase

Mechanistic pathway

Halide

## ABSTRACT

A series of dinuclear  $[Zn_2(L1)_2X_2]$  (**1–3**) and mononuclear  $[Zn(HL2)X_2]$  complexes (**4–6**), ( $X = Cl, Br, I$ ) were synthesised from two Mannich-base compartmental ligands, namely [bis(2-methoxyethyl)amino-methyl]-4-chlorophenol (HL1) and 2,6-bis[bis(2-methoxyethyl)aminomethyl]-4-chlorophenol (HL2), respectively. They were characterised by routine physicochemical techniques (CHN, UV, IR, ESI-MS and NMR) and complex **2–5** was further structurally characterised by single crystal X-ray analysis where the Zn...Zn bond-distance is 3.10–3.12 Å. All the quintessential complexes exhibit excellent phosphatase activity and the experimental first order rate constant values ( $k_{cat}$ ) for the hydrolysis of 4-nitrophenyl phosphate ester (PNPP) reaction in methanol are in the range from 1.05 to 214 s<sup>-1</sup> at 25 °C evaluated by monitoring spectrophotometrically the gradual release of *p*-nitrophenolate ( $\lambda_{max} = 427$  nm,  $\epsilon = 18500$  M<sup>-1</sup> cm<sup>-1</sup>). The coordinated X halides affect the phosphatase activity in the order Br > Cl > I (in dinuclear complexes) and Cl > Br > I (in mononuclear) and the trend in the two cases has been well recognised to be due to a different rate determining step. Moreover the influence of chloro atom in *para*-position of the phenol ring and the role of solvent have been rationalised by comparing the kinetic parameters with those obtained for the corresponding methyl analogues having reasonably close structural resemblance as reported by Sanyal et al. (2014).

© 2015 Published by Elsevier Ltd.

## 1. Introduction

Among the model metalloenzymes studied till date, those containing zinc(II) constitute by far the widest category [1,2]. Indeed, there has been a remarkable success in the identification of zinc-dependent enzymes attributing to emerging crystallographic and spectroscopic techniques [3]. As a matter of fact, each of the fundamental enzyme class, namely, oxidoreductases, transferases, hydrolases, lyases, isomerases, and ligases, is a benchmark of a zinc(II) active site [4–6]. Undoubtedly, phosphatase activity is one of the outstanding functions among the versatile range of enzymatic behaviour of divalent zinc ion [7–10] paving the path for an extensive study of various functional mimics of phospho-esterases. Over the years, synthetic Zn(II) (and also other transition metal) complexes have been judiciously studied as phosphate ester models taking into account their extraordinary Lewis acidity, redox rigidity, nucleophile generation, leaving group stabilization and physiological relevancy [11,12]. However, among the numerous

catalytically promiscuous Zn(II) derivatives [13–29] some complexes show low activity, others require rigorous synthetic conditions or have high toxicity. Therefore the development of new efficient metalocatalysts is still a tough challenge in the field of biocatalysis.

The aim of this work is neatly directed to expand the comprehension of the structure–function relationship of zinc-based model systems showing phosphatase activity (Scheme 1). Recently we have reported that mono- and dinuclear Zn(II) complexes derived from two novel synthesised Mannich-base ligands are not only capable of promoting the hydrolysis of activated phosphate monoesters, but likewise were found to possess promising catalytic activity [30]. In this context, here we report the synthesis and characterisation of a series of similar methoxyamine based mono- and dinuclear Zn<sup>II</sup> complexes, where the ligands differ from those previously reported for the presence in *para* position of the phenol ring of a chloro instead of a methyl group (Scheme 2). The electronic effects of the substituent in *para*-position and of the solvent in which the hydrolysis is carried out have been evaluated. More importantly, a possible mechanism for the PNPP cleavage promoted by Zn<sub>2</sub>L and the concomitant halide role is proposed on the basis of kinetic and spectral analysis.

\* Corresponding authors.

E-mail addresses: [zangrando@units.it](mailto:zangrando@units.it) (E. Zangrando), [dasdebasis2001@yahoo.com](mailto:dasdebasis2001@yahoo.com) (D. Das).



25 °C):  $\delta$  = 2.88 (t, 8H; N-CH<sub>2</sub>-CH<sub>2</sub>), 3.08 (s, 12H; O-CH<sub>3</sub>), 3.42 (t, 8H; N-CH<sub>2</sub>-CH<sub>2</sub>), 3.97 (s, 4H; ph-CH<sub>2</sub>-N), 6.55 (d, 2H; Ar), 7.23 (d, 2H; o to CH<sub>2</sub>-N), 8.01 ppm (s, 2H; o to phenolic-OH); <sup>13</sup>C NMR (300 MHz, DMSO-*d*<sub>6</sub>, 25 °C):  $\delta$  = 52.61 (2C, O-Me), 56.35 (1C, ph-CH<sub>2</sub>-N), 58.04 (2C, N-CH<sub>2</sub>-CH<sub>2</sub>), 69.55 (2C, N-CH<sub>2</sub>-CH<sub>2</sub>), 117.39 (1C, Ar), 122.84 (1C, Ar), 127.13 (1C, Ar), 128.59 (1C, Ar), 129.45 (1C, Ar), 154.93 (1C, Ar-OH); ESI-MS *m/z*: Calcd for [C<sub>13</sub>H<sub>20</sub>ClBrNO<sub>3</sub>Zn]<sup>+</sup> = 419.044, Found = 419.59; FT-IR data (KBr pellet):  $\gamma$  bar = 661, 1268, 1470, 1592 cm<sup>-1</sup>.

### 2.3.3. [Zn<sub>2</sub>(L1)<sub>2</sub>I<sub>2</sub>] (3)

Anhydrous zinc iodide (0.5 mmol, 319.19 mg) in methanol (5 mL) was added dropwise to a methanolic solution (10 mL) of the ligand L1 (0.5 mmol, 136 mg), and the mixture was stirred for 2 h. The resulting yellow solution was filtered. Single crystals suitable for X-ray diffraction experiment were collected after the evaporation of solution.

Yield = 163 mg (70%). Elemental analysis calcd for C<sub>26</sub>H<sub>38</sub>Cl<sub>2</sub>N<sub>2</sub>I<sub>2</sub>O<sub>6</sub>Zn<sub>2</sub>: C, 33.58; H, 4.12; I, 27.29; Cl, 7.62; N, 3.01; O, 10.32; Zn, 14.06; found: C, 33.48; H, 4.27; N, 3.06; I, 27.31; Cl, 7.66; O, 10.28; Zn, 13.94%; <sup>1</sup>H NMR (300 MHz, DMF-*d*<sub>7</sub>, 25 °C):  $\delta$  = 2.86 (t, 8H; N-CH<sub>2</sub>-CH<sub>2</sub>), 3.06 (s, 12H; O-CH<sub>3</sub>), 3.39 (t, 8H; N-CH<sub>2</sub>-CH<sub>2</sub>), 3.95 (s, 4H; ph-CH<sub>2</sub>-N), 6.79 (d, 2H; Ar), 7.28 (d, 2H; o to CH<sub>2</sub>-N), 8.19 ppm (s, 2H; o to phenolic-OH); <sup>13</sup>C NMR (300 MHz, DMSO-*d*<sub>6</sub>, 25 °C)  $\delta$  = 52.66 (2C, O-Me), 56.34 (1C, ph-CH<sub>2</sub>-N), 58.03 (2C, N-CH<sub>2</sub>-CH<sub>2</sub>), 69.50 (2C, N-CH<sub>2</sub>-CH<sub>2</sub>), 117.42 (1C, Ar), 122.89 (1C, Ar), 127.03 (1C, Ar), 128.55 (1C, Ar), 129.48 (1C, Ar), 154.97 (1C, Ar-OH); ESI-MS *m/z*: Calcd for [C<sub>13</sub>H<sub>20</sub>ClINO<sub>3</sub>Zn]<sup>+</sup> = 466.134, Found = 465.98; FT-IR data (KBr pellet):  $\gamma$  bar = 665, 786, 835, 879, 957, 1022, 1109, 1185, 1470, 1590, 2884 cm<sup>-1</sup>.

### 2.3.4. [Zn(HL2)Cl<sub>2</sub>] (4)

To a solution of ligand HL2 (1 mmol, 418 mg) in acetonitrile (25 mL), anhydrous ZnCl<sub>2</sub> (2.5 mmol, 340.5 mg) dissolved in acetonitrile (10 mL) was added and refluxed for 30 min. The mixture was filtered and kept in a beaker for slow evaporation. Colourless rectangular crystals, formed after 2 weeks, were washed with ether to obtain single crystals of good crystallographic quality.

Yield = 327 mg (59%). Elemental analysis calcd for C<sub>20</sub>H<sub>35</sub>N<sub>2</sub>Cl<sub>3</sub>O<sub>5</sub>Zn: C, 43.26; H, 6.35; Cl, 19.16; N, 5.04; O, 14.41; Zn, 11.78; found: C, 43.28; H, 6.41; N, 5.11; Cl, 19.09; O, 14.35; Zn, 11.76%. <sup>1</sup>H NMR (300 MHz, DMF-*d*<sub>7</sub>, 25 °C):  $\delta$  = 2.78 (t, 8H; N-CH<sub>2</sub>-CH<sub>2</sub>), 3.31 (s, 12H; O-CH<sub>3</sub>), 3.50 (t, 8H; N-CH<sub>2</sub>-CH<sub>2</sub>), 4.02 (s, 4H; ph-CH<sub>2</sub>-N), 6.98 ppm (s, 2H; Ar); <sup>13</sup>C NMR (300 MHz, DMSO-*d*<sub>6</sub>, 25 °C):  $\delta$  = 52.44 (4C, O-Me), 56.42 (2C, ph-CH<sub>2</sub>-N), 58.20 (4C, N-CH<sub>2</sub>-CH<sub>2</sub>), 69.58 (4C, N-CH<sub>2</sub>-CH<sub>2</sub>), 117.30 (1C, Ar), 127.13 (2C, Ar), 129.33 (2C, Ar), 1 55.59 (1C, Ar-OH); ESI-MS *m/z*: Calcd for [C<sub>20</sub>H<sub>35</sub>Cl<sub>2</sub>N<sub>2</sub>O<sub>5</sub>Zn]<sup>+</sup> = 520.03, Found = 520.03; FT-IR data (KBr pellet):  $\gamma$  bar = 665, 786, 833, 882, 958, 1020, 1112, 1271, 1471, 1593, 2933 cm<sup>-1</sup>.

### 2.3.5. [Zn(HL2)Br<sub>2</sub>] (5)

It was synthesised by the same procedure as for complex 4 by using zinc bromide. Suitable colourless rhombic-shaped single crystals were obtained for X-ray data collection.

Yield = 367 mg (57%). Elemental analysis calcd for C<sub>20</sub>H<sub>35</sub>N<sub>2</sub>Br<sub>2</sub>ClO<sub>5</sub>Zn: C, 37.29; H, 5.48; N, 4.35; Br, 24.81; Cl, 5.50; O, 12.42; Zn, 10.15; found: C, 37.33; H, 5.43; N, 4.29; Br, 24.83; Cl, 5.51; O, 12.49; Zn, 10.12%. <sup>1</sup>H NMR (300 MHz, DMF-*d*<sub>7</sub>, 25 °C):  $\delta$  = 2.77 (t, 8H; N-CH<sub>2</sub>-CH<sub>2</sub>), 3.34 (s, 12H; O-CH<sub>3</sub>), 3.48 (t, 8H; N-CH<sub>2</sub>-CH<sub>2</sub>), 4.07 (s, 4H; ph-CH<sub>2</sub>-N), 6.97 ppm (s, 2H; Ar); <sup>13</sup>C NMR (300 MHz, DMSO-*d*<sub>6</sub>, 25 °C):  $\delta$  = 52.49 (4C, O-Me), 56.40 (2C, ph-CH<sub>2</sub>-N), 58.25 (4C, N-CH<sub>2</sub>-CH<sub>2</sub>), 69.55 (4C, N-CH<sub>2</sub>-CH<sub>2</sub>), 117.28 (1C, Ar), 127.18 (2C, Ar), 129.35 (2C, Ar), 155.66 (1C, Ar-OH); ESI-MS *m/z*: Calcd for [C<sub>20</sub>H<sub>35</sub>ClBrN<sub>2</sub>O<sub>5</sub>Zn]<sup>+</sup> = 564.12, Found = 565.09;

FT-IR data (KBr pellet):  $\gamma$  bar = 664, 785, 833, 1019, 1111, 1270, 1470, 1592, 2932 cm<sup>-1</sup>.

### 2.3.6. [Zn(HL2)I<sub>2</sub>] (6)

It was also synthesised by following the same method as for complex 4 by using zinc iodide. A colourless crystalline compound of good transparency was obtained and well characterised.

Yield = 502 mg (68%). Elemental analysis calcd for C<sub>20</sub>H<sub>35</sub>N<sub>2</sub>I<sub>2</sub>ClO<sub>5</sub>Zn: C, 32.54; H, 4.78; N, 3.79; I, 34.38; Cl, 4.80; O, 10.84; Zn, 8.87; found: C, 32.58; H, 4.76; N, 3.84; I, 34.41; Cl, 4.77; O, 10.80; Zn, 8.84%. <sup>1</sup>H NMR (300 MHz, DMF-*d*<sub>7</sub>, 25 °C):  $\delta$  = 2.78 (t, 8H; N-CH<sub>2</sub>-CH<sub>2</sub>), 3.31 (s, 12H; O-CH<sub>3</sub>), 3.50 (t, 8H; N-CH<sub>2</sub>-CH<sub>2</sub>), 4.02 (s, 4H; ph-CH<sub>2</sub>-N), 6.98 ppm (s, 2H; Ar); <sup>13</sup>C NMR (300 MHz, DMSO-*d*<sub>6</sub>, 25 °C):  $\delta$  = 52.44 (4C, O-Me), 56.45 (2C, ph-CH<sub>2</sub>-N), 58.21 (4C, N-CH<sub>2</sub>-CH<sub>2</sub>), 69.54 (4C, N-CH<sub>2</sub>-CH<sub>2</sub>), 117.32 (1C, Ar), 127.17 (2C, Ar), 129.37 (2C, Ar), 155.60 (1C, Ar-OH); ESI-MS *m/z*: Calcd for [C<sub>20</sub>H<sub>35</sub>ClINO<sub>5</sub>Zn]<sup>+</sup> = 611.21, Found = 612.37; FT-IR data (KBr pellet):  $\gamma$  bar = 641, 761, 1117, 1197, 1458, 1589, 2877 cm<sup>-1</sup>.

## 2.4. X-ray data collection

Data collection for compounds 2–5 were carried out at room temperature on a Bruker Smart Apex diffractometer equipped with CCD and monochromatized Mo K $\alpha$  radiation ( $\lambda$  = 0.71073 Å). Cell refinement, indexing, and scaling of the data sets were done by using the Bruker Smart Apex and Bruker Saint packages [31]. An absorption correction was applied to all the data sets [32]. The structures were solved by direct methods and subsequent Fourier analyses and refined by the full-matrix least squares method based on *F*<sup>2</sup> with all observed reflections [33]. The  $\Delta F$  map of 3 revealed a disordered methoxy group O(6)–C(34), which could not be suitably modelled. Crystal of 5 (of small dimensions) was low diffracting, but attempts to obtain crystals of better quality were fruitless. Hydrogen atoms were fixed at geometrical positions. All the calculations were performed using the WinGX System, Ver 1.80.05.37 [34].

## 2.5. Kinetic measurements of the hydrolysis of PNPP in methanol

Disodium (4-nitrophenyl)phosphate hexahydrate (PNPP) was used as substrate and the solvents chosen for this study were aqueous DMF and methanol. The solutions of substrate PNPP and Zn complexes in each solvent were freshly prepared maintaining the total volume of the reaction mixture at 2 mL. An initial screening of the hydrolytic propensities of all the metal-complexes was performed till the formation of 2% of *p*-nitrophenolate (~2 h) before to collect kinetic data. The hydrolysis rate of PNPP in the presence of complexes 1–6 was measured by an initial rate method following the absorption increase at 427 nm due to the released 4-nitrophenolate ion in aqueous DMF ( $\epsilon$ , 18500 M<sup>-1</sup> cm<sup>-1</sup>) at 25 °C. All the spectra were recorded for 2 h from a solution containing 1 mmol PNPP and 0.05 mmol Zn complex. Kinetic experiments were performed both at excess substrate and excess Zn complex keeping constant the other conditions. Herein we report only the former data. The study comprised 5 sets having catalyst of 0.05 mmol and substrate concentration of 0.5 (10 equiv), 0.7 (14 equiv), 1.0 (20 equiv), 1.2 (24 equiv) and 1.5 mmol (30 equiv). The reactions were initiated by injecting 0.04 mL of metal complex (2.5 × 10<sup>-3</sup> M) into 1.96 mL of PNPP solution, and the spectrum was recorded only after fully mixing at 25 °C. The visible absorption increase was recorded for a total period of 30 min at regular intervals of 5 min. All measurements were performed in triplicate, and the average value was assumed. The reactions were corrected for the degree of ionisation of the 4-nitrophenol at 25 °C using its molar extinction coefficient at 427 nm. The final *A*<sub>∞</sub> value for each set was obtained after 2 days (at 25 °C).

### 3. Results and discussion

#### 3.1. Synthetic aspects and characterisation of compounds

The “end-off” compartmental ligands used in this work are pure Mannich-type bases and have been synthesised almost by the same procedure as described in our previous work [30], which reports the first observations on anomalous Mannich ligand reaction. The precursors *p*-chlorophenol, bis(2-methoxyethyl)amine and formalin were mixed together under appropriate conditions and refluxed for a prolonged period of time. However certain alterations were detected in the ratio of the component reactants. For the monocondensation reaction, the ratio implemented was 1:0.9:0.9 while the dicondensation pathway required 1:2.2:2.2 that can be attributed to two opposing factors. First and foremost, *p*-chlorophenol is a deactivated benzene ring. It is much less prone to electrophilic substitution reaction as compared to *p*-cresol and obviously it requires a greater concentration of electrophile. On the other hand there is an increasing tendency of getting mixture of the two compounds that makes column chromatographic separation very tough. Thus single-side condensed product (HL1) was almost purely isolated by employing the components in the ratio as mentioned above. Further purification of ligand definitely needs crucial separation by column chromatography. The complexes were synthesised by using anhydrous zinc-halide salts, where the halides were chloro, bromo and iodo. Ligand HL1 gives rise to pentacoordinated dinuclear Zn<sup>II</sup>-complexes (**1–3**) with two halides in a pseudo centrosymmetric arrangement (despite being clearly mononucleating), while the other apparent dinucleating ligand turns out to form mononuclear complexes (**4–6**) as depicted in Fig. 1. This is undeniably an anomalous observation since HL1 is an ideal ligand for the synthesis of mononuclear metalocomplexes and at the same time HL2 is a conventional dinucleating ligand [35–40]. Thus it would not be an overestimation to remark that these kind of Mannich-base compartmental ligand system will generate reverse nuclearity pattern with zinc-halides [30]. Unfortunately, complex **1** and **6** could not be structurally established by repeated endeavours.

Comparing the IR spectra of these compounds to the spectra of analogous compounds and available literature data on metal compounds with a coordination environment comprised of ligands relevant to the present study, viz., of other Mannich and reduced Schiff-base complexes, fairly reliable empirical assignments could be derived for the characteristic IR bands observed for these compounds. The IR spectra of the ligands (Figs. S1 and S2 in Supporting information) and complexes (Figs. S3–S8 in Supporting information) indicate a sharp signal at  $\sim 1100\text{ cm}^{-1}$  for C–N stretching vibration and  $\sim 1580\text{ cm}^{-1}$  for benzene skeletal vibration. Thus it has been proved that these type of ligands can afford kinetically and thermodynamically stable di- and

mono-nuclear complexes with one or two coordination sites on each metal centre, available for substrate binding in appropriate fashion.

Thus here we have chosen the Mannich-based symmetrical dinuclear and unsymmetrical zinc(II) complexes possessing pendant ethylmethoxy chelating arms to investigate the hydrolysis mechanisms of phosphomonoester PNPP. The chloro group at the terminus of the phenolic “end-off” compartmental ligand has been chosen appropriately for the sake of interesting comparative analysis.

#### 3.2. NMR spectral characterisation of ligands and complexes

The ligands (Figs. S9–S12, Supporting information) and complexes (Figs. S13–S16, Supporting information) have been characterised by both proton and carbon NMR spectroscopy in CDCl<sub>3</sub> and DMSO-*d*<sub>6</sub> solvent, respectively. The basic difference in the aromatic region of the two ligands is that the abnormal Mannich product, HL1, displays three signals owing to three non-equivalent protons while the conventional Mannich product shows one peak which can be ascribed to the two equivalent aromatic protons in the benzene ring.

#### 3.3. UV–Vis spectra

The absorption spectra of the ligands in DMF (Supporting information, Fig. S17) show one/two higher energy bands of high intensity in the region 200–250 nm which is attributed to the intraligand charge transfer of the open and closed forms of hydrogen-bonded species. In addition a lower energy band ( $\sim 280\text{ nm}$ ) of lower intensity owing to the zwitterionic form of the ligand. The corresponding spectra in methanol are shown in Fig. S18. The spectra in methanol and DMF can be distinguished by the fact that two high energy band is observed in methanol while it is one for DMF solvent.

The complexes display one/two intraligand charge transfer band(s) around 250–287 nm (high energy) and a ligand to metal charge transfer band at 290–350 nm (low energy) in DMF which is probably due to  $\text{PhO}^- \rightarrow \text{Zn}^{\text{II}}$  or to a mixture of the former and  $\text{X}^- \rightarrow \text{Zn}^{\text{II}}$  (Fig. 2). The spectra remain almost unaffected when measured in excess methanolic solution and therefore is not given separately. The solid-state absorption spectra of the complexes exhibit peaks in the same region (Supporting information, Fig. S19). All the UV-bands and their molar extinction coefficients are tabulated in a list in Table S1 in Supporting information.

#### 3.4. ESI-MS study

To elucidate the structure of the complexes in solution and the active species present in the catalytic pathway during phosphomonoester hydrolysis, the electrospray-ionisation mass spectrometry of the complexes has been performed in the positive mode. The mass spectra of pure complexes, recorded in DMF medium (actually a mixture of DMF–dichloromethane), show a prominent base peak at  $m/z$  374.691 for complex **1** and at  $m/z$  520.03 for complex **4**, as shown in Figs. S20 and S21, respectively. The dinuclear complexes were found to dissociate into two mononuclear moieties; and we report only the mass spectrum of **1** ( $[\text{C}_{13}\text{H}_{20}\text{NO}_3\text{Cl}_2\text{Zn}]^+$ , theoretical  $m/z = 374.601$ ), while for mononuclear series, a single halide ion gets disconnected from the zinc centre to give rise to a unipositive species as proved by the spectrum of complex **4** ( $[\text{C}_{20}\text{H}_{35}\text{N}_2\text{O}_5\text{Cl}_2\text{Zn}]^+$ , theoretical  $m/z = 396.83$ ). In order to get an accurate picture of the structure of the enzyme–substrate adduct in the phosphatase process and the nature of binding of PNPP to the Zn<sup>II</sup>-complexes, we have done further ESI-MS investigations. The mixture solutions of complex and PNPP of ratio 1:100, run

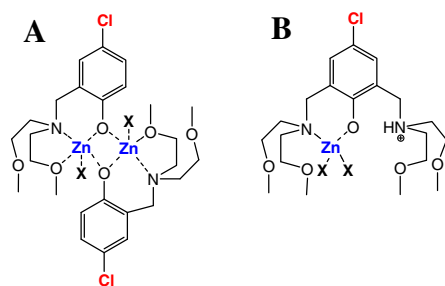


**Fig. 1.** Chemical drawing of the complexes synthesised from ligands HL1 and HL2. (A) 2:2 dinuclear metal-complex  $[\text{Zn}_2(\text{L1})_2\text{X}_2]$  (**1–3**) and (B) 1:1 mononuclear metal-complex  $[\text{Zn}(\text{HL2})\text{X}_2]$  (**4–6**), X = Cl<sup>−</sup> (**1, 4**), Br<sup>−</sup> (**2, 5**), I<sup>−</sup> (**3, 6**).

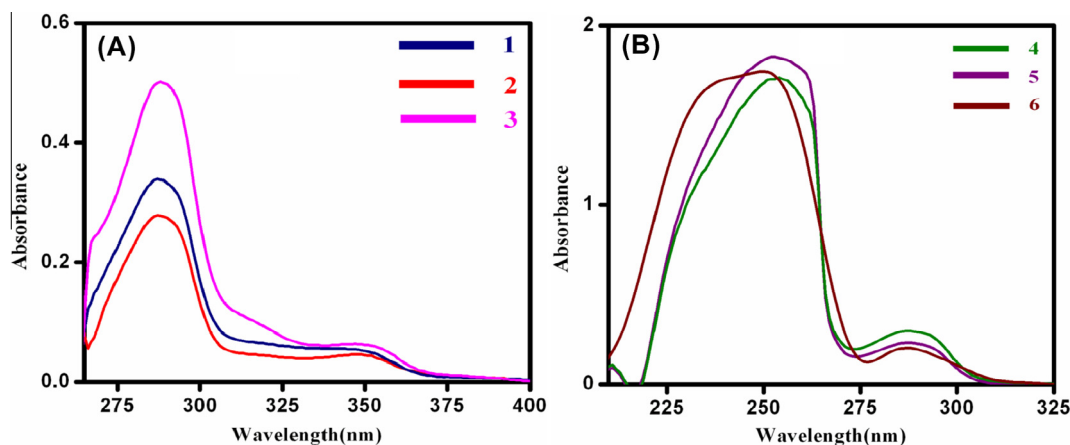


Fig. 2. UV-Vis spectra of the metal-complexes **1–3** (A) and **4–6** (B) in DMF at  $5 \times 10^{-5}$  M concentration.

after 10 min of mixing in methanol solvent, showed the arising of new peaks. In case of **1** a peak detected at 633.48 can be ascribed to the cationic species  $[\text{C}_{20}\text{H}_{27}\text{N}_2\text{O}_{10}\text{ClPZnNa}_2]^+$  (theoretical  $m/z = 633.141$ ) where a substrate molecule is attached to the catalyst in monodentate fashion along with a methanolic moiety (Fig. S22). For **4**, a similar adduct is trapped by mass spectral analysis which gives a signal at 778.56, assigned to the complex cation  $[\text{C}_{27}\text{H}_{42}\text{N}_3\text{O}_{12}\text{ClPO}_{12}\text{ZnNa}_2]$  (theoretical  $m/z = 778.325$ ) as shown in Fig. S23. In both the cases, the pure zinc(II) complex is maintained in solution along with the adducts formed with PNPP.

### 3.5. Solution state structures

The structure of the  $\text{Zn}^{\text{II}}$  complexes in solution as concluded from the ESI-MS investigations is depicted in Fig. 3. It is evident that the dinuclear complexes (**1–3**) dissociates into two equivalent monomeric species, while the mononuclear derivatives (**4–6**) remain intact except for the loss of one of the coordinating halide ions. The molar conductance values (as supplied in Table S2, Supporting information) also support the above fact by proving that they are non-electrolytes.

### 3.6. Thermal analyses

Thermal analyses of all the six complexes have been performed in order to (i) compare their thermal stability by understanding their thermal decomposition patterns, (ii) to verify the molecular composition of the complexes, and (iii) to synthesise the thermally stable end products. The analyses performed in the temperature range 30–700 °C suggest that all of them are stable up to nearly 180 °C. All of them yield ZnO as thermally stable end product. Figs. S24–S26 and S27–S29 depict the thermogram of dinuclear complexes **1–3** and mononuclear complexes **4–6**, respectively. Table 1 reports the calculated and experimental weight losses, temperature range of decomposition for all the complexes studied.

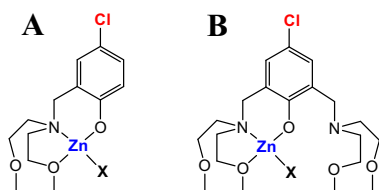


Fig. 3. Chemical drawing of the probable structures of the complexes (A) **1–3**, (B) **4–6** in solution.

The initial temperature  $T_i$  of decomposition of dinuclear and mononuclear zinc complexes follow the trend  $1 > 2 > 3$  and  $4 > 5 > 6$  indicating highest thermal stability of Zn-chloro complex irrespective of the nuclearity of the system. It may be due to better match in size and energy of atomic orbitals between Zn and Cl with respect to other halogens.

### 3.7. Crystal structure determinations

#### 3.7.1. Dinuclear complexes **2** and **3**

The X-ray structural analysis revealed that in complex **2** the metal ions are bridged by two phenolato units in a centrosymmetric fashion forming a four-membered  $\text{Zn}_2\text{O}_2$  core (ORTEP drawing shown in Fig. 4). Complex **3** shows a similar geometry although it lacks a crystallographic centre of symmetry (Fig. 5). A selection of coordination bond lengths and angles is reported in Tables S3 and S4.

In each complex the Zn atoms complete their coordination sphere with the amino nitrogen, a halide and an oxygen from one of the methoxyethyl arms, in a distorted trigonal bipyramidal geometry for which a trigonality  $\tau$  index [41] of 0.53 is derived for **2** and **3**. Thus the Mannich ligand acts as a chelating tridentate species towards a Zn ion, and in addition the phenoxo oxygen connects the metal of another unit, so that one methoxyethyl arm at each ligand remains uncoordinated. In complex **3** one methoxyethyl chain evidences disorder and large thermal ellipsoids for its atoms. Due to the local symmetry, the halide ligands as well as the amine N atoms are trans located with respect to the  $\text{Zn}_2\text{O}_2$  rhomboid mean plane.

In **2–3** the Zn–N and Zn–O distances show decreasing values ongoing from the bromo to the iodo derivative (Table S3). However, it is worth noting that the Zn–O(2) bond distances (involving the coordinated methoxy group) are significantly longer by 0.2–0.3 Å with respect to the other Zn–O distances of the bridging phenolato oxygens. On the other hand, as expected the Zn–halide bond lengths augment from 2.3427(6) to 2.525–2.522(3) Å in **2** and **3**, respectively. The coordination geometry of Br and I derivatives **2** and **3** (the latter with two independent Zn ions has a lower accuracy) appears to follow a trend similar to the corresponding dinuclear complexes synthesised from *p*-cresol recently reported [30]. Thus the electronic property of 4-chlorophenol ( $pK_a = 9.43$ ), a weaker base compared to the *p*-cresol ( $pK_a = 10.26$ ), does not seem to affect the coordination bond distances in the present complexes with respect to the series of methyl analogues. Finally, the Zn–Zn distances are slightly longer (3.1254(8) and 3.101(3) Å, in **2** and **3**, respectively) confirming a short value for the iodine derivative.

**Table 1**  
Theoretical and experimental weight loss of the complexes (from thermogram).

Complex	End product (assumed)	Initial temperature of decomposition (in °C)	End temperature (in °C)	Theoretical weight loss (%)	Experimental weight loss (%) (from thermogram)
1	ZnO	220	630–640	79.2818	85.4046
2		210		89.0011	87.753
3		190		86.20868	82.6209
4	ZnO	190	660	90.3578	83.0179
5		180		87.3752	94.57
6		170		88.2368	97.3885

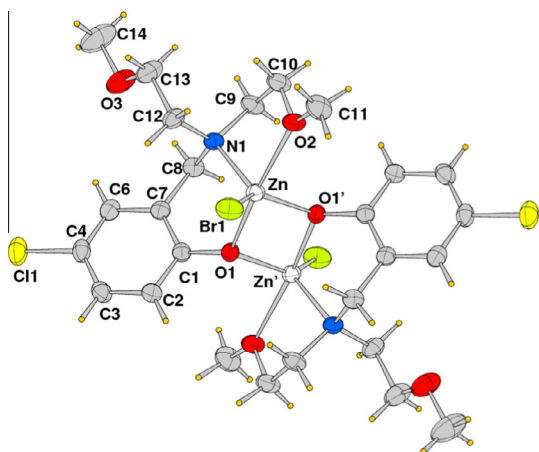


**Fig. 4.** ORTEP view (35% ellipsoid probability) of compound **2** with atom labels of crystallographic independent part.

### 3.7.2. Mononuclear complexes **4** and **5**

The mononuclear entity of complexes **4** and **5** was verified by X-ray structural analysis. The compounds are isomorphous and an ORTEP view of these is shown in **Figs. 6 and 7**, respectively. The metal in both the complexes presents a distorted tetrahedral coordination environment being chelated by the Mannich ligand through the phenolato oxygen and amino nitrogen and in addition by two monocoordinated halides. On the other hand the ethyl-methoxy fragments of the organic ligands point far away and do not interact with the metal centre. The Zn–O and Zn–N bond lengths are close comparable within their esd's being of 1.9408(14) and 1.937(5) Å and 2.0917(17)–2.096(5) Å, in **4** and **5**, respectively, despite the different halide bound at zinc atom (**Table S5**). The chelating angle N(1)–Zn–O(1) of ca. 94° deviates

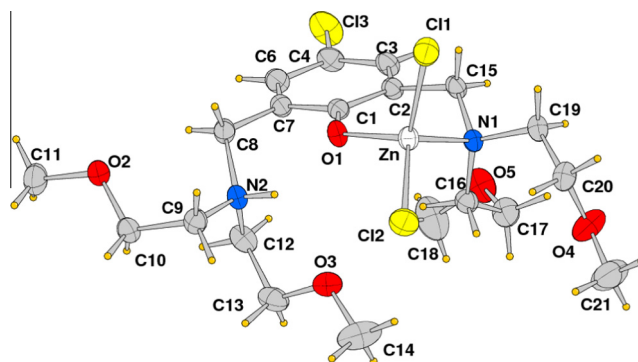


**Fig. 6.** ORTEP view (35% ellipsoid probability) of compound **4**.

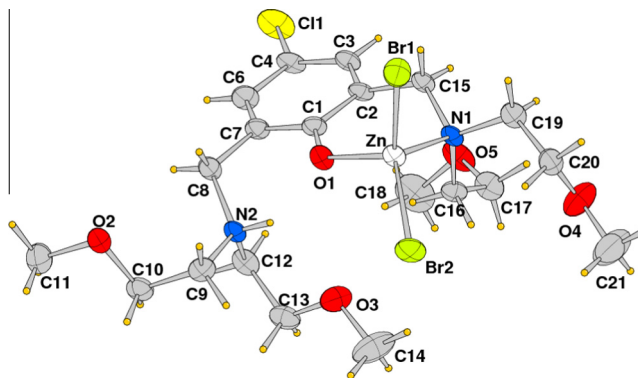


**Fig. 7.** ORTEP view (35% ellipsoid probability) of compound **5**.

significantly from the ideal tetrahedral value, while the other coordination angles in the two complexes are in the range 106.92(5)–116.24(5)°. The metal ion resides almost in the phenolato plane and the coordinated amino nitrogen is displaced by ca. 0.24 Å from it. The structural determination confirms that the amino nitrogen on the other arm of the ligand is protonated and impedes the coordination of a second metal ion. Complex **4** is isomorphous and thus close comparable to the *p*-cresol derivative reported [30]. The protonated nitrogen is at 2.68 Å in both cases from the phenolato oxygen favouring an intramolecular interaction (**Table S6**). The crystal packing does not show any peculiar feature. The crystallographic data and details of refinement for complexes are listed in **Table 2**.

### 3.8. Phosphatase activity

The efficiency of phosphatase activity of the complexes was determined by using the phosphomonoester, *p*-nitrophenylphosphate (PNPP), a common substrate reported in previous investigations. While the study was performed in methanol solvent, the complex was dissolved and added in DMF for solubility reasons. We have deliberately avoided a drastic solvent and in this study

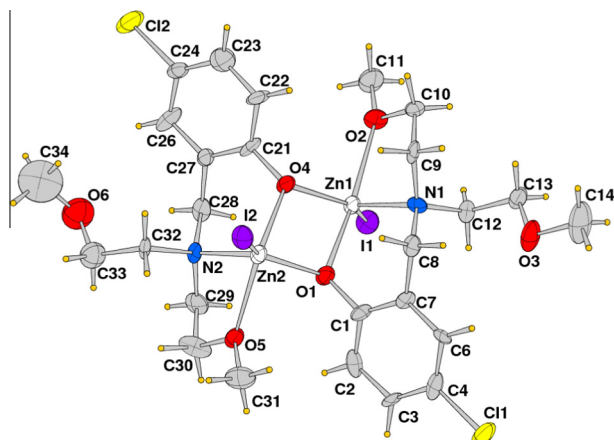


**Fig. 5.** ORTEP view (35% ellipsoid probability) of compound **3**.

**Table 2**  
Crystallographic data and details of refinement for complexes 2–5.

	2	3	4	5
Empirical formula	C <sub>26</sub> H <sub>38</sub> Br <sub>2</sub> Cl <sub>2</sub> N <sub>2</sub> O <sub>6</sub> Zn <sub>2</sub>	C <sub>26</sub> H <sub>38</sub> Cl <sub>2</sub> I <sub>2</sub> N <sub>2</sub> O <sub>6</sub> Zn <sub>2</sub>	C <sub>20</sub> H <sub>35</sub> Cl <sub>3</sub> N <sub>2</sub> O <sub>5</sub> Zn	C <sub>20</sub> H <sub>35</sub> Br <sub>2</sub> ClN <sub>2</sub> O <sub>5</sub> Zn
Fw	836.04	930.02	555.22	644.14
Crystal system	monoclinic	triclinic	triclinic	triclinic
Space group	P2 <sub>1</sub> /c	P $\bar{1}$	P $\bar{1}$	P $\bar{1}$
a (Å)	9.8712(14)	10.134(3)	9.1482(4)	9.285(3)
b (Å)	7.9016(12)	10.886(5)	9.5543(4)	9.699(3)
c (Å)	21.320(3)	15.148(6)	16.5944(7)	16.762(6)
$\alpha$ (°)	90.0	85.109(14)	83.508(2)	83.871(4)
$\beta$ (°)	96.794(2)	87.185(14)	87.016(2)	87.107(4)
$\gamma$ (°)	90.0	82.346(11)	63.9680(10)	63.486(4)
V (Å <sup>3</sup> )	1651.3(4)	1649.0(12)	1294.92(10)	1343.1(8)
Z	2	2	2	2
D <sub>calc</sub> (g cm <sup>-3</sup> )	1.681	1.873	1.424	1.593
$\mu$ (Mo K $\alpha$ ) (mm <sup>-1</sup> )	4.074	3.529	1.289	4.019
F(000)	840	912	580	652
$\theta$ range (°)	1.92–26.54	1.35–21.92	1.23–27.04	1.22–22.98
No. of reflections collected	10785	5330	18946	5308
No. of independent reflections (R <sub>int</sub> )	3159 (0.0319)	3642 (0.0476)	5578 (0.0263)	3481 (0.0406)
No. of reflections (I > 2 $\sigma$ (I))	2384	2064		2731
Refined parameters	181	366	287	283
Goodness-of-fit (F <sup>2</sup> )	1.039	1.036	1.040	1.037
R <sub>1</sub> , wR <sub>2</sub> (I > 2 $\sigma$ (I)) <sup>a</sup>	0.0314, 0.0663	0.0732, 0.1943	0.0358, 0.0946	0.0613, 0.1637
Residuals (e/Å <sup>3</sup> )	0.579, -0.427	1.821, -0.945	0.481, -0.274	1.350, -1.069

$$^a R_1 = \sum ||F_o| - |F_c|| / \sum |F_o|, wR_2 = [\sum w(F_o^2 - F_c^2)^2 / \sum w(F_o^2)^2]^{1/2}.$$

the hydrolytic activity of the complexes was estimated in a common solvent like methanol. Initial measurements for the hydrolysis were run in 97.5% DMF–water solvent mixture, the same used in the previous study with methyl *para*-substituted complexes [30]. However the result patterns were almost the same as those previously reported under similar experimental conditions. The hydrolysis of PNPP was conveniently monitored through UV–Vis spectrophotometry by following the increase of absorbance of the band at 427–430 nm corresponding to the production of 4-nitrophenolate. The preliminary activity of complexes 1–6 were examined by following the protocol earlier reported [30]. The wavelength scan of the complexes were recorded as a mixture of complex and PNPP where the substrate was 20-fold that of the complex in methanol for 2 h at regular time intervals of 10 min as illustrated in Fig. 8 for complex 2 (Figs. S30–S34 in Supporting information for five other complexes).

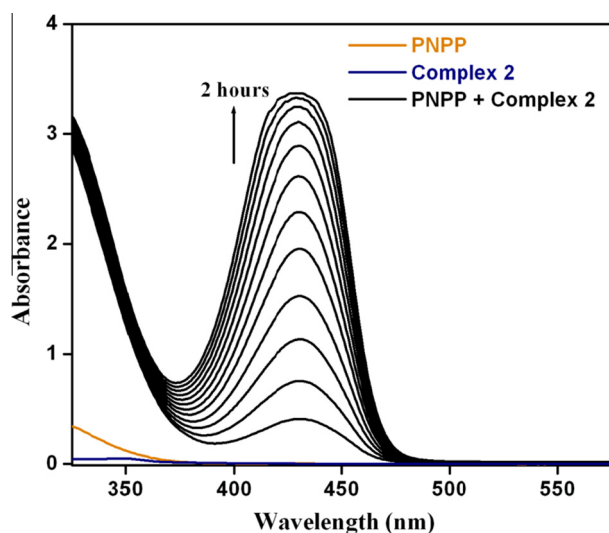


**Fig. 8.** Wavelength scan for the hydrolysis of PNPP in the absence and presence of complex 2 (substrate:catalyst = 20:1) in methanol recorded at 25 °C at an interval of 10 min for 2 h. [PNPP] =  $1 \times 10^{-3}$  M, [Complex] =  $0.05 \times 10^{-3}$  M. The arrow shows the change in absorbance with reaction time.

The absorption profile of the complex–PNPP reaction mixture at the  $\lambda_{\max}$  nearing about 430 nm is represented in Fig. 9 for complex 2 and the others in Supporting information, Figs. S35–S39. It shows that the pathway follows a sigmoidal increase in absorbance as the rate of increase decreases as the reaction approaches to a point of maximum conversion. But this S-shaped nature of the graph does not remain intact for complex 4 and 5 as the rate of increase in absorbance remains equal over the time range of 2 h. The catalytic activity on the hydrolysis of PNPP ester was investigated although the complexes 1–6 in their present structure do not possess any potential nucleophile like metal-coordinated water molecule. Despite the matter that the methyl compounds had shown an extraordinary mechanism for phosphatase activity (in DMF), it was predicted that in case of methanol solvent, the two Zn(II) ions would work cooperatively in the hydrolytic mechanism, through a bridging interaction of the phosphate substrate with the two metals and a simultaneous nucleophilic attack of a Zn–OH function on the substrate by the addition of an external water molecule on one of the zinc ions. But the results point towards a different story where the nature of nucleophilic reagent is probably a methanolic group instead of a water molecule.

### 3.9. Control experiments

Control experiments have been performed in order to examine whether there is any role of the ligand used for metallation and the metal-salt themselves in the hydrolytic activity shown. We arrive at the result that the metal-complex is solely responsible for the phosphatase activity, i.e., the catalysis is zinc-ion mediated. The control experiments are represented in Fig. S40 (A, B and C) in Supporting information. Although the control with zinc-halide metal-salts tend to portray a band maxima at near about 430 nm, we can consider it as too negligible to be taken into account.

### 3.10. Kinetics

The accumulated kinetic data were analysed on the basis of Michaelis–Menten equation. The enzymatic kinetics plot (substrate–catalyst interdependence) and the double-reciprocal plots are shown in Fig. 10 for complex 2 and for the rest of the

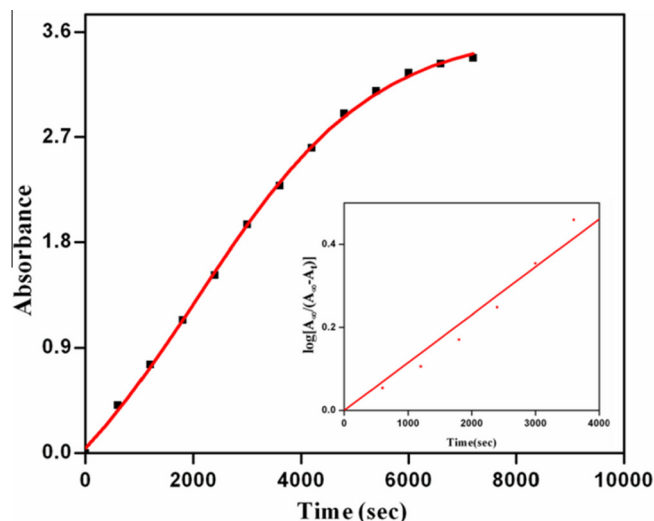


**Fig. 9.** Absorption profile on addition of PNPP to complex **2** due to the formation of *p*-nitrophenolate ( $\lambda_{\text{max}} = 427 \text{ nm}$ ) monitored for 2 h. Inset shows the plot of  $\log [A_{\infty} / (A_{\infty} - A_t)]$  vs. time for 1 h ( $R^2 = 0.955$ , standard deviation = 764.5).

complexes in Figs. S41–S45 in Supporting information. The first-order rate constant values are given in Table 3 and the rest of the parameters are supplied in Table S7 in Supporting information. The kinetic results indicate that the degree of catalytic power of the complexes in methanol follows the order of  $2 > 1 > 3 > 6 > 5 > 4$ . Thus there are two vital points to be emphasised from the trend: firstly, the dinuclear complexes (**1–3**) are more reactive than the mononuclear ones (**4–6**), as previously anticipated. Secondly, the halide effect is not homogeneous in the two group of complexes, being  $\text{Br} > \text{Cl} > \text{I}$  in case of the dinuclear complexes (Fig. 11A) while the trend for mononuclear is  $\text{I} > \text{Br} > \text{Cl}$  (Fig. 11B).

### 3.11. Mechanistic implications

The coordination patterns and binding models of the catalyst–substrate complex have been largely explored in literature [15,16,20,30,42] and after rigorous considerations two plausible catalytic cycles having reasonably good agreement with our kinetic

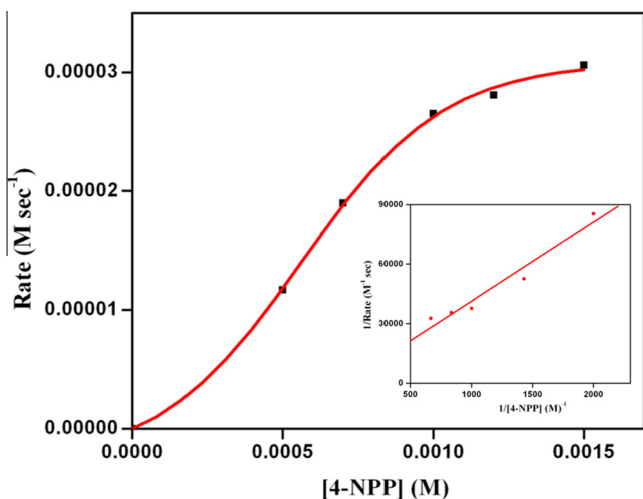


**Fig. 10.** Plot of enzymatic kinetics for complex **2** ( $V$  vs.  $[S]$ ). Inset shows the Lineweaver–Burk plot ( $1/V$  vs.  $1/[S]$ ) having intercept = 93.5806 (error = 9.11), slope = 3.9859 (error = 0.7129),  $R^2 = 0.955$  and standard deviation = 764.54.

**Table 3**

First order rate constant values ( $\text{s}^{-1}$ ) for phosphatase activity of complexes **1–6** in the present in our previous study (Ref. [30]).

Complex	$k_{\text{cat}}$ ( $\text{s}^{-1}$ )	$k_{\text{cat}}$ ( $\text{s}^{-1}$ ) values of analogous <i>para</i> -substituted methyl derivatives (Ref. [30])
<b>1</b>	8.94	9.35
<b>2</b>	13.06	8.88
<b>3</b>	5.10	8.33
<b>4</b>	1.05	4.68
<b>5</b>	1.79	3.29
<b>6</b>	4.35	2.88

results have been postulated from the previous representative mechanisms. The substrate molecule binds as a dianionic mononitrophenyl phosphate to the complex having phosphatase activity. An altered mechanism of hydrolysis for the metal-complexed phosphate monoester have been demonstrated for the methanol as compared to the reaction pathway in DMF solvent as reported earlier [30]. As depicted in Fig. 12, for the mononuclear series of complexes (**4–6**), RDS is the one where halide ion gets dissociated from the metal-centre after the addition of PNPP which is probably in a bidentate fashion. A methanol molecule gets associated with the  $\text{Zn}^{\text{II}}$  ion leading to the intermediate **III** which is deprotonated to yield a methoxide ion as the potent nucleophile in our case (intermediate **IV**). **IV** has been identified in ESI-MS study as a major signal at an  $m/z$  of 778.56. It is followed by the formation of an organophosphorus intermediate by nucleophilic substitution reaction with the concomitant expulsion of 4-nitrophenolate ion. It then gradually breaks down into the original complex and phosphoric acid. In case of dinuclear complexes (**1–3**), the picture is slightly different in the perspective that the addition of PNPP and dissociation of halide ion occurs in a simultaneous fashion, i.e., in a well-concerted pathway, as vividly represented in Fig. S46 in Supporting information. The complex–substrate adduct is attacked by a methanol molecule and that intermediate has been successfully trapped by electrospray-ionisation mass spectrometry providing an obvious peak at  $m/z$  633.48 which is followed by a similar series of reactions to complete the catalytic cycle. Thus the initial phosphorylation rate is straight-away portrayed in the experimental rate constant magnitude.

Clearly, we have assumed a bipoint binding mode in the key step of the pathway over a monopoint addition picture. Now some intrinsic questions concerning the phosphatase mechanism arises in our mind, such as (i) what is the special advantage in forming the phosphoryl intermediate for indirect hydrolysis and (ii) how does an external methanol molecule associated with the  $\text{Zn}^{\text{II}}$  ion become a nucleophile over the internally present methoxy group? This can be attributed to the fact that after the substrate has been recognised and associated via coordination linkages and electrostatic interactive forces, a proper coordination pattern grows up whereby the configuration is just ideal for a nucleophilic attack from the metal-centre to the electrophilic phosphorus site. It is only after that step that a chain of events follow by which 4-nitrophenolate gets departed from the reaction-complex which proves that substrate coordination is a general pre-requisite. Moreover, the conjugate-base of *p*-nitrophenol is a very weak base and hence *p*-nitrophenolate is a poor leaving group and so direct hydrolysis would never proceed in absence of a phosphoryl intermediate. The second point raised although seems contradictory to the fact that intramolecular reactions are always preferred over intermolecular reactions, is quite justified from this perspective that the methoxy group suffers a considerable amount of steric hindrance in our coordination sphere than the methanol moiety or any other general base and hence lacks sufficient flexibility to attack the phosphorus atom embedded in the cavity throughout the reaction ordinate. Therefore that possibility is clearly ruled

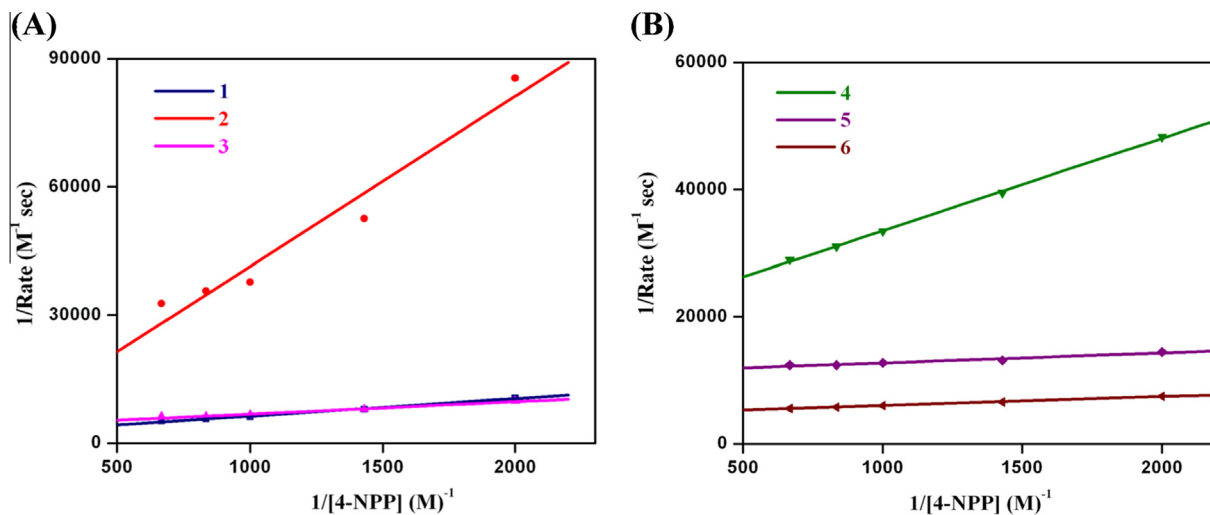


Fig. 11. Overlay of the Lineweaver–Burk curves of (A) dinuclear complexes 1–3 and (B) mononuclear ones 4–6.

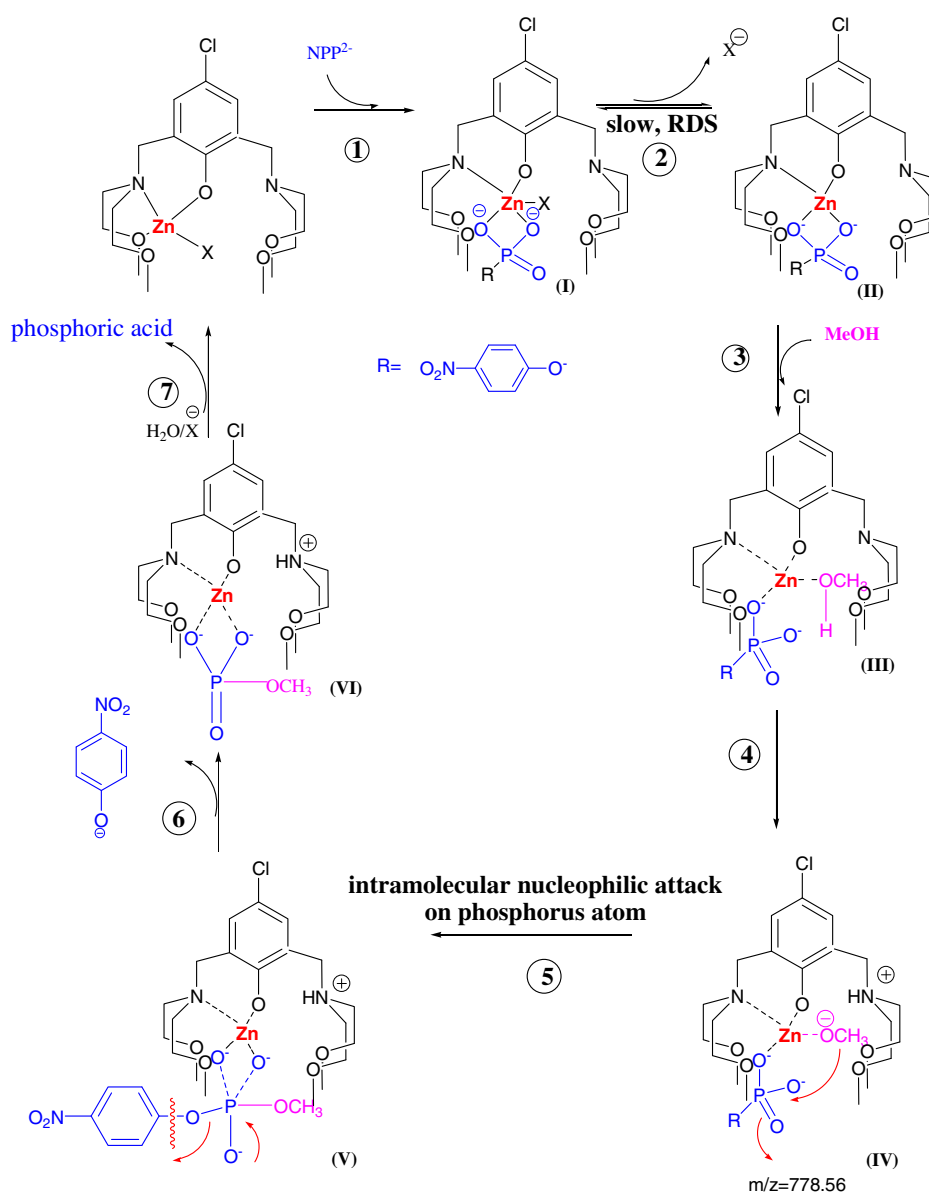


Fig. 12. Plausible mechanism for PNPP hydrolysis promoted by mononuclear complexes 4–6.

out as it appears to be electronically and geometrically fictitious as demonstrated in Fig. 13. Here it is necessary to say that a methanolic nucleophile is more accurate than a classical aqueous nucleophilic reagent despite the fact that the  $pK_a$  value of the two are very comparable ( $pK_{a, \text{water}} = 15.7$ ,  $pK_{a, \text{MeOH}} = 16$ ), since we have avoided any deliberate inclusion of water in any proportion to our catalytic system. The above postulated mechanistic pathway is reasonably consistent with, and can be used to systematically interpret, the experimental observations reached in our case.

The dinuclear compounds are expectedly more catalytically active than their mononuclear analogues [43–47,24,48], although the former provide effectively mononuclear species in solution. This is primarily due to the fact that the total concentration of catalytically active species is twice in case of dinuclear complexes independent of the halide ion. Many literature studies have explored coordinating ligands that act to sterically constrain the  $Zn^{II}$  geometry, therefore limiting the extent of the geometrical flattening for appropriate enzyme–substrate interaction. In our case, the steric factor acts only in case of ligand HL2 due to the second methoxyethyl chelating arm which is the secondary reason for the lower reactivity of the mononuclear compounds as compared to the dinuclear ones.

Thus if we compare our catalytic activity results with that of our previous work by Sanyal et al. [30] (Table 3), we observe specific changes, both qualitatively and quantitatively, viz., there is a huge change in the nature of halide dependence on kinetic behaviour and the rate constant value of complex 2 which is a dinuclear complex of HL1 and  $ZnBr_2$  metal-salt. The overlay of the Line-weaver Burk plots of the ten complexes (1, 3–6 from both series) generated by Michaelis Menten analysis has been represented in Fig. 14A and complex 2 has been plotted separately in Fig. 14B since 2 of chloro series has an extremely high catalytic efficiency. Although the dual-point binding model has been kept unaltered, there have been complete change in the nature of solvent used along with the alteration in the *para*-group. Previously we had opted for 97.5% DMF which is roughly a non-aqueous catalytic medium, the catalytic amount of water present in the system is potent enough to render nucleophilicity for solvolysis of P–O bond. So there occurs a basic change in the actual nucleophile participating in the catalysis. Now the magnitude of rate of hydrolysis, in terms of  $k_{\text{cat}}$  values, is essentially lower than the methyl-compounds except in two cases, which are complex 2 and 6. This is probably because DMF being an aprotic but highly polar solvent can stabilise the ionic intermediates to a larger extent than methanol solvent by ion–dipole interaction. However methanol can display some amount hydrogen-bonding interaction which cannot exceed the degree of stabilisation attained from ion–dipole interaction. The discrepancy which is shown for 2 and 6 must be for the chloro-group in the *para*-position of the benzene ring which activates the metal-catalyst by its electron-withdrawing inductive effect and renders the zinc-ion more Lewis-acidic making the hydrolytic assay much more favourable. The  $Zn \cdots Zn$  intermetallic bond-distances of the two series of complexes have not been dealt with for comparative

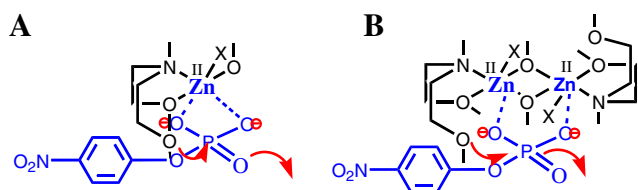


Fig. 13. Possible intermediates with the methoxy group as the effective nucleophile during phosphatase activity promoted by (A) dinuclear complexes 1–3 (B) and mononuclear ones 4–6.

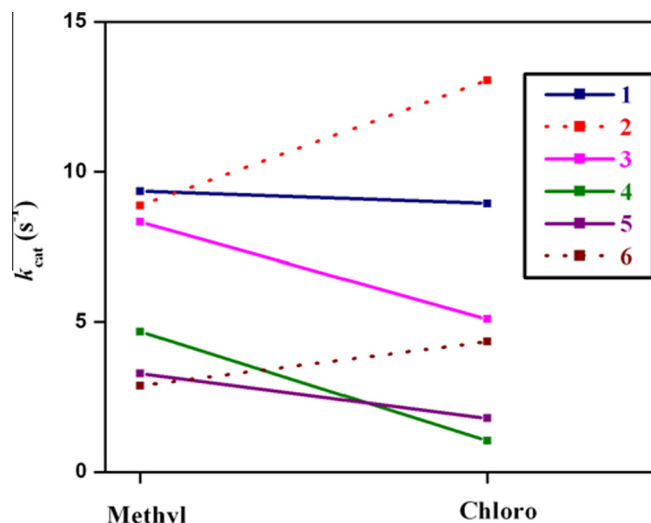


Fig. 14. Overlay of the Lineweaver–Burk plots of complexes 1–6 with those of the methyl analogues in our previous work.

study since the bimetallic complexes tend to dissociate into mononuclear entities and lose their dimeric nature in the process.

### 3.12. Influence of electronegativity and bond energy

There are two governing parameters which rule the phosphatase activity of zinc-halido metal-complexes, namely electronegativity trend and the zinc–halogen bond energy value. The electronegativity factor influences the reaction rate in a fashion such that the pathway should be preferred for the coordinated halide which is more electronegative and this is because the more electronegative halide increases the Lewis acidity of the zinc metal ion (Fig. S47). In the later case, the bond energy value is inversely proportional to the rate since higher value implies poorer leaving group ability (Fig. S48). A conclusion which should be apparent from the foregoing is that both these parameters are meaningful in determining the catalytic power of a complex and our observations are a combination of both these characteristic property. A similar situation did not arise for the methyl-substituted complexes where only electronegativity factor ruled the entire kinetics and it was computationally verified. The matter is very complicated to elucidate the reason behind the relative governance of these two proposed factors where the possibility of a substantial solvent role cannot be ruled out which needs further theoretical modelling.

## 4. Conclusions

The cleavage of phosphoester PNPP mediated by Mannich-based di- and mononuclear zinc(II) complexes have been investigated. It has been discussed that although monomeric entities can perform as active catalyst, the dinuclear ones are more competitive than their mononuclear counterparts in P–O bond-fission. To accommodate all the kinetic data, we have established that while the dinuclear catalysts prefer a concerted catalytic mechanism, the mononuclear counterparts religiously follow a step-wise  $S_N2$ -type nucleophilic addition–substitution pathway. Conclusively, this research definitely provides certain insights into the solvent effect, halide role, nuclearity influence and their interrelation in synthetic phosphatase model zinc complexes with Mannich base ligands leading to a more or less perfect functional mimic. Although no absolute correlation could be drawn between

the topological architecture of a molecule and its efficiency of phosphoester hydrolysis, few accumulated facts appear salient and define the crucial factors in designing efficient artificial phosphatases. In particular, we can end this project in this noble anticipation that the knowledge acquired is quite satisfactory to obtain more attractive phosphoesterase mimics in the future. Finally, these being Zn(II) compounds provide a rational alternative to expensive, less abundant, and more toxic heavy-metal-containing complexes. We can end here with this note that though this field has attracted significant research attention, a lot more job remains behind.

### Conflict of interest

Authors declare that there are no conflicts of interests.

### Acknowledgements

This research is funded by the Council of Scientific and Industrial Research, New Delhi [CSIR project No. 01(2464)/11/EMR-II dated 16-05-2011 to D.D.]. R.S. is thankful to CSIR-SRF fellowship for financial support.

### Appendix A. Supplementary data

CCDC 1022805–1022808 contains the supplementary crystallographic data for complex 2–5. These data can be obtained free of charge via <http://www.ccdc.cam.ac.uk/conts/retrieving.html>, or from the Cambridge Crystallographic Data Centre, 12 Union Road, Cambridge CB2 1EZ, UK; fax: +44 1223 336 033; or e-mail: [deposit@ccdc.cam.ac.uk](mailto:deposit@ccdc.cam.ac.uk).

Supplementary data associated with this article can be found, in the online version, at <http://dx.doi.org/10.1016/j.poly.2015.05.013>.

### References

- [1] D.E. Wilcox, *Chem. Rev.* 96 (1996) 2435.
- [2] L.J. Daumann, G. Schenk, D.L. Ollis, L.R. Gahan, *Dalton Trans.* 43 (2014) 910.
- [3] B.L. Vallee, D.S. Auld, *Acc. Chem. Res.* 26 (1993) 543.
- [4] M. Hambidge, N. Krebs, *J. Pediatr.* 135 (1999) 661.
- [5] (a) G.A. Eby, *J. Antimicrob. Chemother.* 40 (1997) 483; (b) A. Gadomski, *J. Am. Med. Assoc.* 279 (1998) 1999; (c) M.L. Macknin, M. Piedmonte, C. Calendine, J. Janosky, E. Wald, *J. Am. Med. Assoc.* 279 (1998) 1962; (d) M.L. Cleveland Macknin, *Clin. J. Med.* 66 (1999) 27; (e) D.G. Barceloux, *J. Toxicol. Clin. Toxicol.* 37 (1999) 279; (f) E.J. Petrus, K.A. Lawson, L.R. Bucci, K. Blum, *Curr. Ther. Res.* 59 (1998) 595; (g) N.K.A. Bakar, D.M. Taylor, D.R. Williams, *Chem. Speciation Bioavail.* 11 (1999) 95; (h) D.R. Williams, *Coord. Chem. Rev.* 186 (1999) 177.
- [6] G. Parkin, *Chem. Rev.* 104 (2004) 699.
- [7] M.J. Jedrzejak, P. Setlow, *Chem. Rev.* 101 (2001) 607.
- [8] M. Subat, K. Woinaroschy, C. Gerstl, B. Sarkar, W. Kaim, B. König, *Inorg. Chem.* 47 (2008) 4661.
- [9] (a) J.G. Zalatan, D. Herschlag, *J. Am. Chem. Soc.* 128 (2006) 1293; (b) J. Weston, *Chem. Rev.* 105 (2005) 2151; (c) F. Mancini, P. Tecilla, *New J. Chem.* 31 (2007) 800; (d) S.D. Aubert, Y. Li, F.M. Rauschel, *Biochemistry* 43b (2004) 5707; (e) J.R. Morrow, *Com. Inorg. Chem.* 29 (2008) 169.
- [10] M.A.R. Raycroft, C. Tony Liu, R.S. Brown, *Inorg. Chem.* 51 (2012) 3846.
- [11] (a) E. Kimura, T. Koike, *Adv. Inorg. Chem.* 44 (1997) 229; (b) J.E. Coleman, *Curr. Opin. Chem. Biol.* 2 (1998) 222.
- [12] B. Bauer-Siebenlist, F. Meyer, E. Farkas, D. Vidovic, S. Dechert, *Chem. Eur. J.* 11 (2005) 4349.
- [13] P. Chakraborty, J. Adhikary, R. Sanyal, A. Khan, K. Manna, S. Dey, E. Zangrando, A. Bauzá, A. Frontera, D. Das, *Inorg. Chim. Acta* 421 (2014) 364.
- [14] P. Kundu, P. Chakraborty, J. Adhikary, T. Chattopadhyay, R.C. Fischer, F.A. Mautner, D. Das, *Polyhedron* 85 (2015) 320.
- [15] S. Anbu, S. Kamalraj, B. Varghese, J. Muthumary, M. Kandaswamy, *Inorg. Chem.* 51 (2012) 5580.
- [16] K. Abe, J. Izumi, M. Ohba, T. Yokoyama, H. Okawa, *Bull. Chem. Soc. Jpn.* 74 (2001) 85.
- [17] S.M. Annigeri, A.D. Naik, U.B. Gangadharmath, V.K. Revankar, V.B. Mahale, *Transition Met. Chem.* 27 (2002) 316.
- [18] A.D. Naik, V.K. Revankar, *Proc. Indian Acad. Sci. (Chem. Sci.)* 113 (2001) 285.
- [19] S. Brooker, T.C. Davidson, *Chem. Commun.* (1997) 2007.
- [20] H. Arora, S.K. Barman, F. Lloret, R.N. Mukherjee, *Inorg. Chem.* 51 (2012) 5539.
- [21] J. Chen, X. Wang, Y. Zhu, J. Lin, X. Yang, Y. Li, Y. Lu, Z. Guo, *Inorg. Chem.* 44 (2005) 3422.
- [22] C. Bazzicalupi, A. Bencini, E. Berni, A. Bianchi, V. Fedi, V. Fusi, C. Giorgi, P. Paoletti, B. Valtancoli, *Inorg. Chem.* 38 (1999) 4115.
- [23] D.P. Goldberg, R.C. diTargiani, F. Namuswe, E.C. Minnihan, S. Chang, L.N. Zakharov, A.L. Rheingold, *Inorg. Chem.* 44 (2005) 7559.
- [24] O. Iranzo, A.Y. Kovalevsky, J.R. Morrow, J.P. Richard, *J. Am. Chem. Soc.* 125 (2003) 1988.
- [25] R. Bonomi, F. Selvestrel, V. Lombardo, C. Sissi, S. Polizzi, F. Mancini, U. Tonellato, P. Scrimin, *J. Am. Chem. Soc.* 130 (2008) 15744.
- [26] C. Vichard, T.A. Kaden, *Inorg. Chim. Acta* 337 (2002) 173.
- [27] L.V. Penkova, A. Macia-g, E.V. Rybak-Akimova, M. Haukka, V.A. Pavlenko, T.S. Iskenderov, H. Kozzowski, F. Meyer, I.O. Fritsky, *Inorg. Chem.* 48 (2009) 6960.
- [28] J. He, J. Sun, Z.-W. Mao, L.-N. Ji, H.J. Sun, *Inorg. Biochem.* 103 (2009) 851.
- [29] L. Zhu, O. Santos, C.W. Koo, M. Rybstein, L. Pape, J.W. Canary, *Inorg. Chem.* 42 (2003) 7912.
- [30] R. Sanyal, A. Guha, T. Ghosh, T.K. Mondal, E. Zangrando, D. Das, *Inorg. Chem.* 53 (2014) 85.
- [31] Bruker, APEX and SAINT programs, Bruker AXS Inc., Madison, Wisconsin, USA, 2007.
- [32] Bruker, SADABS, Bruker AXS Inc., Madison, Wisconsin, USA, 2001.
- [33] G.M. Sheldrick, *Acta Crystallogr.* A64 (2008) 112.
- [34] L.J. Farrugia, *J. Appl. Crystallogr.* 45 (2012) 849.
- [35] H. Sakiyama, R. Mochizuki, A. Sugawara, M. Sakamoto, Y. Nishida, M. Yamasaki, *J. Chem. Soc., Dalton Trans.* (1999) 997.
- [36] H. Sakiyama, A. Sugawara, M. Sakamoto, K. Unoura, K. Inoue, M. Yamasaki, *Inorg. Chim. Acta* 310 (2000) 163.
- [37] H. Sakiyama, R. Ito, H. Kumagai, K. Inoue, M. Sakamoto, Y. Nishida, M. Yamasaki, *Eur. J. Inorg. Chem.* 8 (2001) 2027.
- [38] H. Sakiyama, T. Suzuki, K. Ono, R. Ito, Y. Watanabe, M. Yamasaki, M. Mikuriya, *Inorg. Chim. Acta* 358 (2005) 1897.
- [39] H. Sakiyama, M. Yamasaki, T. Suzuki, Y. Watanabe, R. Ito, A. Ohnishi, Y. Nishida, *Inorg. Chem. Commun.* 9 (2006) 18.
- [40] J. Shibayama, H. Sakiyama, M. Yamasaki, Y. Nishida, *Anal. Sci.: X-ray Struct. Anal. Online* 24 (2008) 177.
- [41] A.W. Addison, T.N. Rao, J. Reedijk, J. van Rijn, G.C. Verschoor, *J. Chem. Soc., Dalton Trans.* (1984) 1349.
- [42] X. Zhang, X. Zheng, D. Lee Phillips, C. Zhao, *Dalton Trans.* (2014), <http://dx.doi.org/10.1039/c4dt01491j>.
- [43] G.N. De Iuliis, G.A. Lawrance, S. Fieuw-Makaroff, *Inorg. Chem. Commun.* 3 (2000) 307.
- [44] T.A. Steitz, J.A. Steitz, *Proc. Natl. Acad. Sci. U.S.A.* 90 (1993) 6498.
- [45] B.W. Pontius, W.B. Lott, P.H. Von Hippel, *Proc. Natl. Acad. Sci. U.S.A.* 94 (1997) 2290.
- [46] L.R. Gahan, S.J. Smith, A. Neves, G. Schenk, *Eur. J. Inorg. Chem.* 19 (2009) 2745.
- [47] C. He, S.J. Lippard, *J. Am. Chem. Soc.* 122 (1999) 184.
- [48] C. Bazzicalupi, A. Bencini, C. Bonaccini, C. Giorgi, P. Gratteri, S. Moro, M. Palumbo, A. Simionato, J. Sgrignani, C. Sissi, B. Valtancoli, *Inorg. Chem.* 47 (2008) 5473.